Permanent dipole moment and first-order hyperpolarizability of Li-induced polarization clusters in $K_{1-x}Li_xTaO_3$ determined by hyper-Raman spectroscopy

H. Vogt
Max-Planck-Institut für Festkörperforschung, Heisenbergstrasse 1, D-70569 Stuttgart, Germany
(Received 5 December 1997; revised manuscript received 3 April 1998)

Hyper-Raman spectra of six samples of $K_{1-x}Li_xTaO_3$ with Li concentrations x between 0.008 and 0.087 are measured in the wave number range below 120 cm^{-1} at temperatures well above the transitions to glassy or ferroelectric-type states. An internal reference method is demonstrated based on a comparison of hyper-Rayleigh and hyper-Raman scattering intensities recorded under identical conditions. With the soft-mode hyper-Raman line being taken as calibration standard, absolute values of the permanent dipole moment and the first-order hyperpolarizability of the polarization clusters around the off-center Li ions are obtained. Although only integrated intensities are involved, our procedure requires a detailed analysis of the spectral broadening of the hyper-Rayleigh line, which exceeds 1 cm^{-1} above 200 K. This analysis yields evidence that hyper-Rayleigh scattering solely results from thermally activated hopping motions of the Li ions and that orientational correlations between the Li ions may be ignored in the high-temperature limit under study. At room temperature our results are $p_{PC}^{*}=18$ D (Debye units) $\hat{=}3.7e$ Å (electron charge times length measured in Å) and $\beta_{222}=1\times10^{-30}$ $g^{-1/2}$ $cm^{7/2}$ s (cgs units) $\hat{=}4\times10^{-40}$ $m^4\,V^{-1}$ (SI units), where p_{PC}^{*} and β_{222} are the effective dipole moment of a polarization cluster and the dominant component of its hyperpolarizability tensor, respectively. Both quantities increase with decreasing temperature and reflect the growth of the polarization clusters due to the slowing down of the soft mode. A temperature-independent intrinsic or core dipole moment $p_{PC}=2.3$ D$\hat{=}0.48e$ Å is deduced from p_{PC}^{*} and discussed with regard to the off-center displacement of the Li ion. [S0163-1829(98)00839-X]

I. INTRODUCTION

In recent years hyper-Rayleigh (HRL) or second-harmonic light scattering has attracted much interest as a straightforward experimental technique for determining the optical second-order polarizability, also called first-order hyperpolarizability, of molecules.[1–3] This quantity describes the simplest nonlinear optical response and is defined as a third-rank tensor β_{ijk} relating the second-order term $\vec{p}^{(2)}$ of the molecular dipole moment to the dyadic square of the local electric field $\vec{E}^{\mathrm{loc}}$ generated by the incident laser radiation, i.e.,

$$p_i^{(2)}=\sum_{j,k=1}^{3}\beta_{ijk}E_j^{\mathrm{loc}}E_k^{\mathrm{loc}}. \tag{1}$$

The internal reference method comparing the molecular hyperpolarizabilities of solute and solvent within a solution[4] has turned out to be particularly useful. Here, the HRL intensity scattered from the solution into a direction perpendicular to the incident laser beam is measured as a function of the solute concentration. Provided the individual molecules act like independent scatterers contributing incoherently to the HRL intensity,[1] a ratio of the form

$$s=\frac{\langle\beta_{\mathrm{solute}}^2\rangle}{\langle\beta_{\mathrm{solvent}}^2\rangle} \tag{2}$$

can be deduced from the linear relationship between HRL signal and number density of the dissolved molecules. The angular brackets in expression (2) denote averages over molecular orientations while β_{solute} and β_{solvent} stand for linear combinations of tensor elements β_{ijk} selected by the scattering geometry and by the transformation between the molecular and the laboratory coordinate systems.[5] In favorable cases, however, both β_{solute} and β_{solvent} are dominated by just one tensor element, so that the orientational averages only yield numerical prefactors and a ratio of hyperpolarizabilities can directly be estimated from expression (2).

Of course, the internal reference method requires the molecular hyperpolarizability of at least one solvent to be known as a calibration standard. Therefore HRL scattering from solutions has to be complemented by the more difficult technique of electric-field-induced second-harmonic generation[6] (EFISHG) in a number of common solvents. In EFISHG the dipolar molecules of the solvent under study are partly aligned by an external static electric field and Maker fringes due to coherent second-harmonic generation (SHG) are measured relative to those of crystals with known SHG susceptibilities. Since the degree of alignment depends on the permanent dipole moment of the molecules, this quantity is involved in the SHG efficiency.[7] Moreover, there is a contribution from the optical third-order polarizability (second-order hyperpolarizability) describing SHG due to a ''mixing'' of the external static electric field and the laser radiation. It is clear that the accuracy by which absolute values of hyperpolarizabilities can be obtained from HRL scattering relies on the availability of all parameters relevant to EFISHG in the solvents used for calibration.

In this paper, a variety of the internal reference method just described is applied to the solid solution $K_{1-x}Li_xTaO_3$ (KLT) in which K ions of the persistently cubic perovskite

$KTaO_3$ are replaced by Li impurities. Since the ionic radii of Li^+ and K^+ differ by a factor of almost two, the Li ion cannot fill the centrosymmetric lattice site of the K ion, but is displaced from the K site by about a quarter of the lattice constant along one of the six equivalent $\langle 100 \rangle$ directions.[8] The off-center displacement is equivalent to the addition of an electric dipole with a moment of almost 5 D [Debye unit $=10^{-18}$ $g^{1/2}$ $cm^{5/2}$ s^{-1} $\hat{=}(1/3)\times 10^{-29}$ C m). In response to this rather strong disturbance there is a local lattice relaxation that we shall call polarization cluster for short, including the Li dipole at its core.

At elevated temperatures the Li ions fluctuate between their six equivalent off-center positions. The dynamics of these thermally activated hopping motions can be characterized by a distribution of relaxation frequencies the center of which follows an Arrhenius law of the form

$$f_0(T) = f_0(\infty)\exp\left\{-\frac{E_b}{k_B T}\right\}, \tag{3}$$

where E_b denotes the height of the energy barrier to be overcome in a 90° flip and $f_0(\infty)$ is the attempt frequency.[9–13] Nearly all studies of KLT have concentrated on the cooperative behavior of the Li dipoles below 100 K, especially on their condensation to a glassy or ferroelectric-type state.[14–16] In this paper, however, attention is restricted to a temperature range well above any phase transition, so that to some degree the Li-induced polarization clusters may be considered as orientationally uncorrelated like the dissolved molecules in a dilution.

The orientational fluctuations of the polarization clusters give rise to HRL scattering. There are two slightly different ways to interpret this phenomenon:

(a) A local first-order hyperpolarizability β_{ijk} is attributed to each polarization cluster. Hence the integrated HRL intensity is determined by some orientational average of the square of this quantity [see expression (2)].

(b) The hopping motions of the Li ions are accompanied by fluctuations of the macroscopic polarization $\vec{P}(\vec{r},t)$ as well as the second-order susceptibility $\chi^{(2)}_{ijk}(\vec{r},t)$ around their vanishing mean values. In the simplest approximation the second quantity is a linear functional of the first one, i.e.,

$$\chi^{(2)}_{ijk}(\vec{r},t) = \chi^{(2)}_{ijk}[\vec{P}(\vec{r},t)] = \sum_{l=1}^{3}\left(\frac{\partial \chi^{(2)}_{ijk}}{\partial P_l}\right)_{\vec{P}=0} P_l(\vec{r},t). \tag{4}$$

Accordingly, the HRL intensity reflects the mean square of the polarization induced in $KTaO_3$ by the Li impurities.

Since $KTaO_3$ preserves its cubic O_h symmetry down to low temperatures, HRL scattering should be absent in the pure host crystal, so that in contrast to molecular solutions an internal reference seems to be missing. It has been shown that in nominally pure samples of $KTaO_3$ symmetry-breaking defects, unavoidable at the present state of the art of crystal growing, lead to HRL scattering, which becomes clearly observable below 50 K when the surrounding polarization clusters cover a sufficiently large number of unit cells.[17,18] This defect-induced HRL scattering, however, cannot be used as an intensity standard for calibrating HRL scattering from KLT because the nature of the defects is difficult to identify and their concentrations can hardly be controlled, so that significant variations among $KTaO_3$ samples grown in different laboratories have been found.[18–20]

A more appropriate effect seems to be EFISHG in $KTaO_3$. It is well characterized[21] and can provide an internal reference for determining the hyperpolarizability of the polarization clusters in KLT by a study of EFISHG as a function of Li concentration. Here, the problem arises that an external electric field affects the alignment of the Li ions to a degree that remains rather unpredictable as long as the magnitudes of the relevant parameters, especially the off-center displacement and dipole moment of the Li impurity, are still a matter of debate.[22]

Therefore it is more promising to take the route via spontaneous hyper-Raman (HRM) scattering by the zone-center soft mode of $KTaO_3$. The absolute cross section or efficiency of this process can be calculated from the coefficients of EFISHG, provided the ion displacement pattern induced by the external field in the EFISHG experiment is dominated by the eigenvector of the soft mode.[23] Using this relation between soft-mode HRM effect and EFISHG, we obtain the hyperpolarizability of the polarization clusters in KLT from a comparison of HRL and HRM scattering intensities. Admittedly, we also have to assume that doping of $KTaO_3$ with Li does not influence the soft-mode HRM tensor, so that the HRM efficiency varies with x only via the x dependence of the soft-mode frequency. Such a simplification is justified if the polarization clusters are isolated from each other, i.e., at elevated temperatures far above the onset of collective behavior.

It is tempting to go one step further and to identify the fourth-rank tensor $\partial\chi^{(2)}_{ijk}/\partial P_l$, introduced in Eq. (4), with the EFISHG coefficients determined for pure $KTaO_3$, P_l being the polarization induced by an external static field in the direction of the lth cubic axis. Now HRL scattering from KLT becomes a property of the host crystal whereas the Li impurities only provide the inhomogeneous polarization $\vec{P}(\vec{r},t)$ necessary for the effect. This idea is not new. It has already been applied by Azzini *et al.*[24] in order to estimate the dipolar correlation length in KLT at low temperatures from SHG experiments, which they have essentially treated as HRL scattering in the forward direction. Moreoever, Voigt and Kapphan[25] have shown that SHG in KLT is well described by attributing a SHG tensor of point group symmetry $4mm$ to each ''dipolar region,'' the tetragonal axis being parallel to the direction of the dipole moment. They found this tensor to agree in the ratios of its components with the EFISHG tensor of pure $KTaO_3$ referring to an electric field in the dipole direction. Expressing their experimental results in our notation, we may state that SHG and HRL scattering in KLT are characterized by a fourth-rank tensor $\partial\chi^{(2)}_{ijk}/\partial P_l$ coinciding at least in its structure and the ratios of its components with the corresponding tensor of EFISHG coefficients of pure $KTaO_3$. In order to understand the relation between Li-induced HRL scattering in KLT and EFISHG in pure $KTaO_3$, we have to realize that the first effect only probes a small-wave-vector Fourier component of the polar local lattice distortions around the symmetry-breaking impurities. Like the displacement pattern due to an external electric field this Fourier component is mainly determined by the soft-mode eigenvector,[18] so that in both

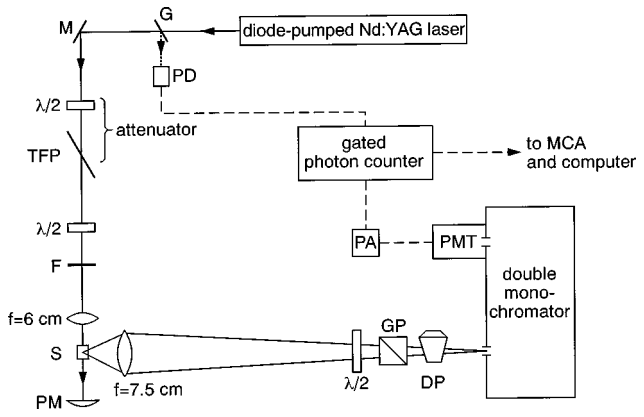

FIG. 1. Experimental setup for observing hyper-Rayleigh and hyper-Raman scattering from $K_{1-x}Li_xTaO_3$ in a 90° scattering geometry. PM, power meter; *S*, sample in cryostat; *F*, Schott filter, RG 850; λ/2, half-wave plate; TFP, thin-film polarizer; *M*, mirror; *G*, glass plate for directing some backreflected laser light on the triggering photodiode PD; GP, Glan prism; DP, Dove prism as image rotator; PMT, photomultiplier tube; PA, preamplifier; MCA, multichannel analyzer.

cases $\partial\chi^{(2)}_{ijk}/\partial P_l$ can be specified as $\partial\chi^{(2)}_{ijk}/\partial P^{\mathrm{SM}}_l$ where P^{SM}_l is the polarization associated with the soft-mode displacements along the *l*th cubic axis. Following Bruce and Cowley,[26] we may also refer to the well-known concept of Huang scattering when pointing out that the essential effect of the Li ions is similar to that of a static or quasistatic local field conjugate to the ordering coordinate of the host, i.e., the normal coordinate or polarization of the soft mode.

As long as the soft-mode HRM tensor can be expressed in terms of EFISHG coefficients and vice versa, it is involved in HRM as well as HRL scattering and can be canceled in the ratio of HRL and HRM intensities. Then the transverse effective charge of the soft mode calculable from the TO-LO splittings of the zone-center phonons[27] acts as a standard to which the dipole moment of the polarization clusters is referred. Thus both hyperpolarizability and permanent dipole moment associated with the off-center Li ions can be deduced from the HRM spectrum measured at a given temperature as a function of x. Several conditions, however, have to be met that require careful consideration.

The outline of the paper is as follows. In Sec. II we describe experimental details and display characteristic results. The line shape of the HRL line is analyzed in Sec. III. We interpret the ratio of HRL and soft-mode HRM intensities in Sec. IV. Finally, in Sec. V we present our estimates of hyperpolarizability and permanent dipole moment of the Li-induced polarization clusters and discuss their significance.

II. EXPERIMENTAL DETAILS AND REPRESENTATIVE RESULTS

The HRM setup is sketched in Fig. 1. The source of the exciting radiation is a diode-laser-pumped Nd-YAG laser (Coherent Model DPY 501 QII). The acousto-optic *Q* switch provides laser pulses of 30-ns width and 3.2-kHz repetition rate. The average power at the site of the sample *S* is about 0.5 W. A combination of a half-wave plate (λ/2) and a thin-film polarizer (TFP) is used as attenuator. All spectra are taken in a 90° scattering geometry, which in Porto's notation can be specified by $X(YY)Z$ where X, Y, and Z stand for the cubic axes of the crystals under study. The scattered light is collected by an $f/1$ objective with a focal length of $f=7.5$ cm. A Dove prism rotates the image of the laser beam passing through the sample, so that it is parallel to the entrance slit of the double monochromator. The image has to exceed the height of the entrance slit in order to exclude the sample surfaces from contributing to the measured signal and to confine the scattering volume to the bulk of the samples.

The six single crystals of KLT under study are generously provided by S. Kapphan (FB Physik, University of Osnabrück, D-49069 Osnabrück, Germany). Their Li concentrations have been determined by NMR and SHG as explained in Ref. 25. All samples have the form of cubes with edges parallel to the ⟨100⟩ axes, the edge lengths varying between 2 and 6 mm. They are mounted on a copper block in a continuous-flow cryostat and cooled by helium exchange gas. Their temperature is controlled within ± 0.1 K.

There are two reasons to make no use of multichannel detection by a position-sensing photomultiplier tube as described in our previous papers,[17,28] but to apply the conventional single-channel technique combining a scanning double monochromator, a Burle/RCA C31034 photomultiplier tube, and a gated photon-counting equipment:

(i) Spectral response and instrumental profile are much simpler because they do not suffer from pixel cross talks and imaging problems.[28]

(ii) The single-channel setup copes more easily with the orders-of-magnitude difference between HRL and HRM intensities at lower temperatures because the HRL intensity can selectively be attenuated by calibrated neutral density filters while the double monochromator is scanning through the HRL line.

The spectral slit width [full width at half maximum (FWHM) of instrumental profile] is chosen to be always $\Delta\tilde{\nu}=2.7$ cm^{-1}. This is a compromise: On the one hand $\Delta\tilde{\nu}$ is small enough to detect the broadening of the HRL line above 200 K, whereas on the other hand, $\Delta\tilde{\nu}$ is large enough to observe HRL scattering up to room temperature even at the lowest Li concentration. In order to determine the instrumental profile and to exclude any contribution from the spectral width of the laser radiation itself, we compare the line shape of the frequency-doubled laser beam with that of a Ne line near 532 nm emitted from a low-pressure discharge lamp. For the given spectral resolution, both line shapes coincide and are well described by a Gaussian.

The typical temperature dependence of the HRM spectrum between -120 cm^{-1} (anti-Stokes side) and $+120$ cm^{-1} (Stokes side) at a given Li concentration x is shown in Fig. 2. With decreasing temperature, three features are noticed: the convergence of the Stokes and anti-Stokes soft-mode HRM lines, the blowup of the HRL intensity, and the narrowing of the HRL line. We remark that variations of the HRL linewidth have not been found in our preceding studies of KLT.[29,30] There, the temperature was always kept below 200 K while at temperatures between 120 and 200 K the spectral slit width was about 3.6 cm^{-1}. It is clear from

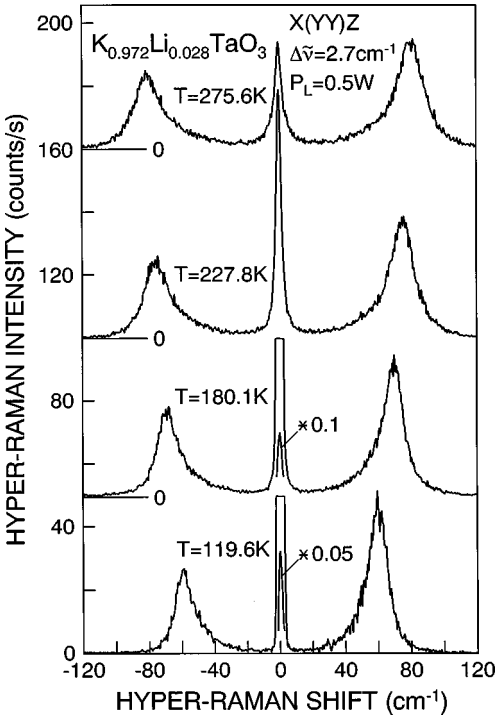

FIG. 2. The low-frequency hyper-Raman spectrum of $K_{0.972}Li_{0.028}TaO_3$ at four different temperatures. The 90° scattering geometry is denoted by $X(YY)Z$, i.e., the incident and scattered light propagate in the [100] and [001] direction, respectively, while the electric fields of both are parallel to the [010] axis. The spectral slit width (FWHM of the instrumental profile) is $\Delta\tilde{\nu}=2.7\ \mathrm{cm}^{-1}$. An average laser power $P_L=0.5$ W at the site of the sample is used. Note the shift of the Stokes and anti-Stokes hyper-Raman lines as well as the narrowing and rapid increase of the hyper-Rayleigh line at the center. In the two lower diagrams, the peaks of the hyper-Rayleigh lines are scaled down by factors of 10 and 20, respectively.

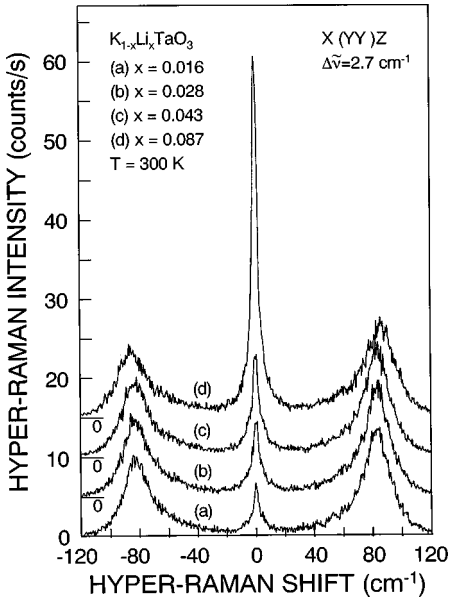

FIG. 3. The room-temperature hyper-Raman spectrum of $K_{1-x}Li_xTaO_3$ as a function of the Li concentration x. Scattering geometry and spectral resolution are those of Fig. 2. The four spectra are scaled, so that their integrated hyper-Raman intensities are the same.

Fig. 2 that under these conditions the broadening of the HRL line remains unresolved.

The x dependence of the HRM spectrum at a given temperature is displayed in Fig. 3. The intensities are scaled to yield the same integral soft-mode intensity for all concentrations. Qualitatively, we can state that the width of the HRL line is independent of x whereas the HRL intensity increases with x. Apparently, however, there is no strictly linear relation between HRL intensity and Li concentration.

For all Li concentrations x and temperatures T under study, the HRM spectrum is described by a spectral function $S(\Omega,x,T)$, which can be written as the sum of three contributions:

$$S(\Omega,x,T)=I_{\mathrm{EL}}(x,T)\,\delta(\Omega)+I_{\mathrm{LR}}(x,T)F_{\mathrm{LR}}(\Omega,x,T)+I_{\mathrm{DHO}}(x,T)F_{\mathrm{DHO}}(\Omega,x,T). \tag{5}$$

Each of the three terms is the product of an integral intensity and a line shape function referred to the whole Ω axis and normalized to 1. In order to reproduce the HRL line, we have to combine a δ function and a Lorentzian given by

$$F_{\mathrm{LR}}(\Omega,x,T)=\frac{\Gamma/2\pi}{\Omega^2+(\Gamma/2)^2}, \tag{6}$$

where $\Gamma=\Gamma(x,T)$ is its FWHM. As normalized line shape function of the damped harmonic oscillator representing the soft mode we use the formula

$$F_{\mathrm{DHO}}(\Omega,x,T)=\frac{1}{\pi}\,\frac{n(\Omega,T)+1}{\tilde{n}(\Omega_0,\gamma,T)+\frac{1}{2}}\,\frac{\Omega_0\gamma\Omega}{(\Omega_0^2-\Omega^2)+\gamma^2\Omega^2}, \tag{7}$$

where $n(\Omega,T)$ is the Bose-Einstein population factor, while $\Omega_0=\Omega_0(x,T)$ and $\gamma=\gamma(x,T)$ denote frequency and damping constant of the soft mode, respectively. As can be verified by contour integration (for example, see Ref. 31), $\tilde{n}(\Omega_0,\gamma,T)$ is given by

$$\tilde{n}(\Omega_0,\gamma,T)=n(\Omega_0,T)-\frac{\Omega_0\gamma}{\pi\omega_T^2}\sum_{m=1}^{\infty}\frac{m}{[m^2+(\Omega_0/\omega_T)^2][m^2+m(\gamma/\omega_T)+(\Omega_0/\omega_T)^2]} \tag{8a}$$

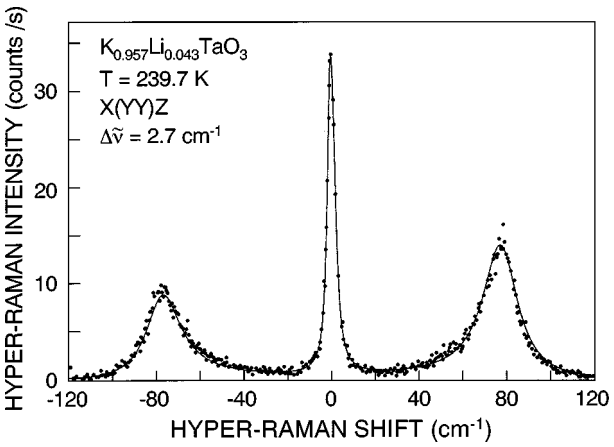

FIG. 4. Six-parameter description of the hyper-Raman spectrum of $K_{0.957}Li_{0.043}TaO_3$ at $T=239.7$ K. The superposition of a damped harmonic oscillator response, a central Lorentzian, and a central δ function is convoluted with the instrumental profile and then fitted to the experimental points. Scattering geometry and spectral resolution are those of Fig. 2. The six fit parameters are defined by Eqs. (4) to (8) and have the values $I_{EL}=26.7$ counts/s, $I_{LR}=6.65I_{EL}$, $I_{HRM}=25.4I_{EL}$, $\Omega_0=77.9$ cm^{-1}, $\gamma=18.9$ cm^{-1}, and $\Gamma=3.8$ cm^{-1}.

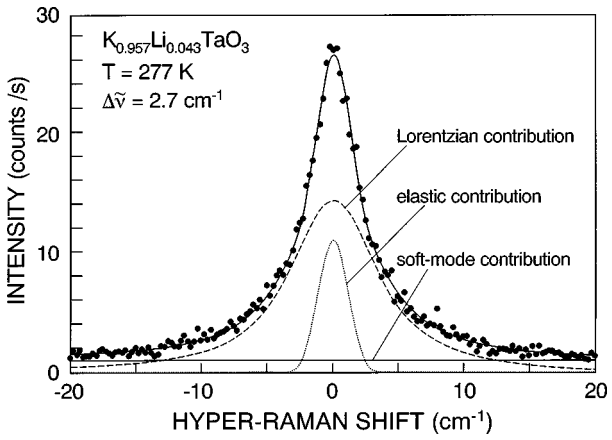

FIG. 5. Decomposition of the hyper-Rayleigh line of $K_{0.975}Li_{0.043}TaO_3$ at $T=277$ K into three contributions arising from soft-mode hyper-Raman scattering, purely elastic, i.e., unresolvable hyper-Rayleigh scattering, and Lorentzian-type quasielastic second-harmonic light scattering. The solid line through the experimental points is the sum of the three curves underneath.

with

$$\omega_T=\frac{2\pi k_B T}{\hbar}. \tag{8b}$$

In the temperature interval of interest, i.e., between 120 and 300 K, the correction of $n(\Omega_0,T)$ by the second term in Eq. (8a) remains almost negligible.

As already mentioned in Ref. 30, the single-oscillator description turns out to be insufficient for the highest Li concentration $x=0.087$ at $T\lesssim 200$ K. Here, Eq. (7) has to be supplemented by the line shape function of a second damped harmonic oscillator of lower frequency and minor weight. This change of line shape is not yet understood since it does not seem to be related to the Li-induced phase transition around 100 K.

The convolution of expression (5) with the instrumental profile is fitted to the experimental data, the fit parameters being I_{EL}, I_{LR}, I_{DHO}, Ω_0, γ, and Γ. The quality of our fitting procedure is demonstrated in Fig. 4. In Fig. 5 we show the decomposition of the HRL line into the contributions from the three terms in Eq. (5). The interpretation of the fit parameters is postponed to the following sections.

III. SPECTRAL BROADENING OF HYPER-RAYLEIGH LINE

The spectral broadening of the HRL line can easily be explained in terms of a Debye relaxator of relaxation frequency $f_0=1/2\pi\tau_0$ modulating the second-order susceptibility $\chi^{(2)}_{ijk}$ according to Eq. (4). Using the fluctuation-dissipation theorem,[32] we obtain the relation

$$S_D(\Omega)\sim[n(\Omega,T)+1]\varepsilon''_D(\Omega), \tag{9}$$

where $S_D(\Omega)$ is the contribution of the Debye relaxator to the spectral function of the scattered second-harmonic light and $\varepsilon''_D(\Omega)$ the imaginary part of its dielectric function. We may write

$$[n(\Omega,T)+1]\approx\frac{k_B T}{\hbar\Omega} \tag{10}$$

and

$$\varepsilon''_D(\Omega)\sim\frac{\Omega\tau_0}{1+(\Omega\tau_0)^2}. \tag{11}$$

Combining Eqs. (9) to (11) and lumping together the factors of proportionality to an integral intensity, we reproduce the Lorentzian term in Eq. (5) with

$$\Gamma=\frac{2}{\tau_0}. \tag{12}$$

In Fig. 6 we plot Γ as a function of temperature. Within the experimental accuracy, a systematic variation of Γ with Li concentration x at a given temperature T cannot be observed, so that Γ has to be taken as independent of x. Therefore we only show the mean value by a full circle and indicate the range in which the values of Γ of all six samples are found by an error bar.

Although the temperature interval in which the spectral broadening of the HRL line can be analyzed is rather small, an Arrhenius law as given by Eq. (3) is well fitted to the experimental data (solid line in Fig. 6). We obtain $E_B/k_B=1000$ K and $f_0(\infty)/c=120$ cm^{-1}. These parameter values are surprisingly close to those derived from dielectric measurements at frequencies below 1 GHz and temperatures below 150 K.

The Arrhenius laws available from the literature[8–15] are displayed in Fig. 7 where they are extrapolated to high temperatures. The results of various authors scatter within the hatched areas. There are two relaxation frequencies characterizing the orientational fluctuations of the Li dipoles. The

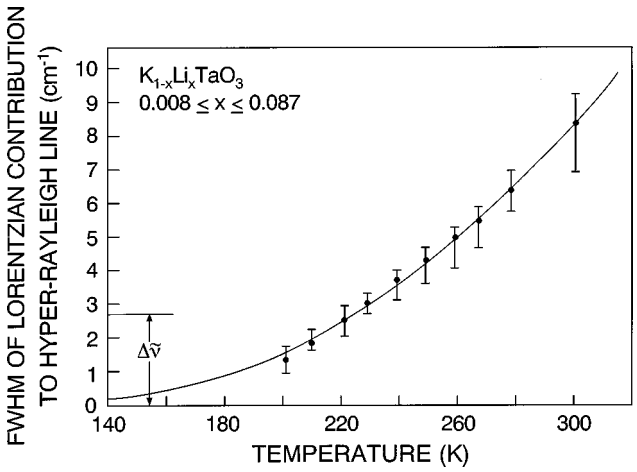

FIG. 6. The width (FWHM) of the Lorentzian contribution to the hyper-Rayleigh line as a function of temperature. Each error bar covers the values of all six samples under study at the given temperature, while the full circle represents the mean value. The solid line is a fit of an Arrhenius law to the experimental points with $E_B/k_B=1000$ K and $f_0(\infty)/c=120$ cm^{-1}. The spectral resolution is indicated by the FWHM $\Delta\tilde{\nu}$ of the instrumental profile.

lower one ($E_B/k_b\approx 2500$ K) is associated with the reorientation of pairs of closely spaced Li ions,[13] sometimes called Li dimers,[12] while the higher one ($E_B/k_B\approx 1000$ K) refers to 90° flips of single Li dipoles becoming cooperative at lower temperatures.[11–13] From Fig. 7 we expect the higher-frequency relaxation mechanism to give rise to a HRL line broadening observable above 240 K if the spectral slit width is around 1 cm^{-1}. The lower-frequency relaxation mechanism, however, should remain unresolved until about 420 K. Taking into account the values of energy barrier and attempt frequency deduced from Fig. 6, we have to conclude that the Lorentzian contribution to the HRL line results from hopping

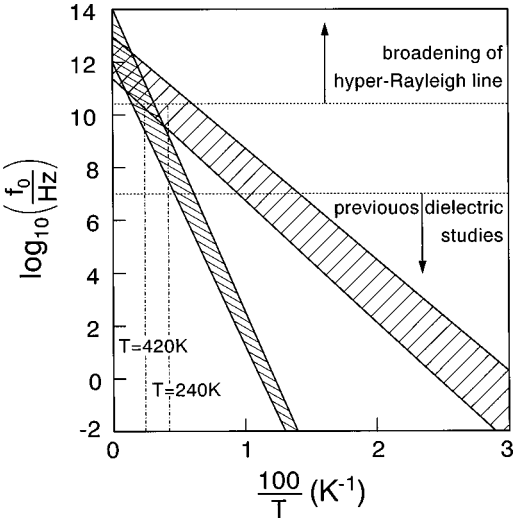

FIG. 7. Temperature dependence of the two relaxation frequencies characterizing the orientational fluctuations of the Li dipoles. The decadic logarithm of $f_0=1/(2\pi\tau_0)$, where τ_0 is the relaxation time, is plotted as a function of the reciprocal temperature. The Arrhenius laws of the form $\ln f_0(T)=A-B/T$ found by various authors are extrapolated to high temperatures and scatter within the hatched areas.

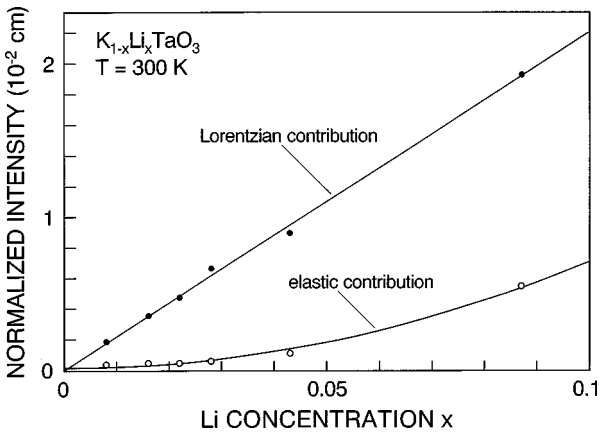

FIG. 8. Normalized intensities of the Lorentzian and the elastic, i.e., unresolved contributions to the hyper-Rayleigh line at room temperature.

motions of almost isolated Li ions, the absence of correlations being indicated by the independence of Γ from x. On the other hand, the purely elastic, i.e., unresolvable contribution to the HRL line is most probably due to Li dimes or more complex agglomerates of impurities becoming noticeable only at higher Li concentrations.

This picture is supported by Fig. 8, which shows the normalized integral intensities I_{LR} and I_{EL} as a function of x at room temperature. The normalization procedure applied will be described in the following section. Like the independence of Γ from x, the linear increase of I_{LR} with x gives evidence that the orientational correlation between the Li ions or their polarization clusters contributing to I_{LR} is negligible. The nonlinearity in the relation between HRL intensity and x as already conspicuous in Fig. 3 is confined to I_{EL}. The quadratic increase of I_{EL} with x is in line with the assumption that I_{EL} arises from Li dimers whose density depends on x^2. According to Fig. 8, there may also be a small, but constant background contribution to I_{EL} resulting from defects besides the Li impurities.

In Fig. 9 we compare the HRL lines of the sample with the lowest Li concentration ($x=0.008$) and a sample of nominally pure $KTaO_3$ (sample 5 in Ref. 18) at room temperature. As in Fig. 3, the intensities are scaled to yield equal integrated soft-mode HRM intensities in both cases. The HRL line shape of nominally pure $KTaO_3$ coincides with the instrumental profile. Therefore no doubt is left that the spectral broadening is induced entirely by the Li ions and that spurious amounts of these dopants can be excluded as sources of HRL scattering or SHG in nominally pure $KTaO_3$.[33] We take the opportunity to point out that the peak intensity of HRL scattering in nominally pure $KTaO_3$ at room temperature does not exceed the order of magnitude of the background soft-mode HRM intensity around $\Omega=0$. This remark is not in conflict with Ref. 25 where much higher HRL intensities have been reported because no particular care was taken to block second-harmonic light scattering at the sample surfaces from contributing to the measured signal.

Finally, we have to note that from the numerical point of view the decomposition of the HRL line into a Lorentzian and an elastic part is somewhat arbitrary. We may just as well introduce a distribution of relaxation times or frequen-

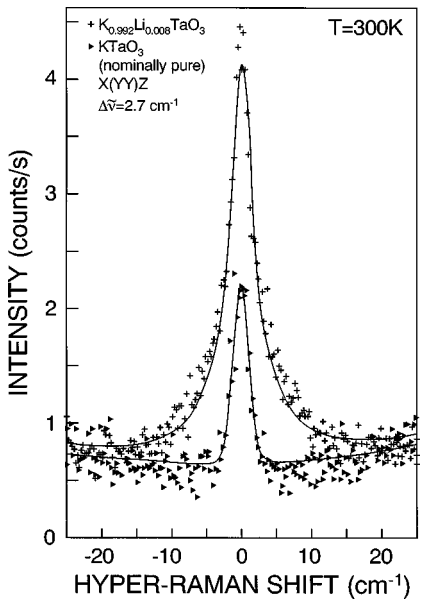

FIG. 9. The weakest hyper-Rayleigh line of this study ($K_{0.992}Li_{0.008}TaO_3$, room temperature) compared with the hyper-Rayleigh line of a sample of nominally pure $KTaO_3$. The two spectra are scaled, so that the integrated soft-mode hyper-Raman intensities are the same and also agree with those of Fig. 3. The solid lines are fits of Eqs. (5)–(8) to the experimental data. Note the absence of the Lorentzian broadening ($I_{LR}=0$) in the case of nominally pure $KTaO_3$.

cies and describe the HRL line shape by an expression of the form

$$S_{HRL}(\Omega)=\frac{I_{HRL}}{\pi}\int_0^\infty d\tau g(\tau)\frac{\tau}{1+(\Omega\tau)^2}. \tag{13}$$

Here, I_{HRL} is the integral HRL intensity and $g(\tau)$ stands for the relaxation-time probability density normalized to 1 and characterized by a mean or center value τ_0 and a width $\Delta\tau$. Referring to previous dielectric measurements, we may choose either a log-normal[9,10] or a beta-type distribution.[12,13] If we replace the first two terms in Eq. (5) by Eq. (13), we only exchange the three parameters I_{EL}, I_{LR}, and Γ by three other ones, i.e., I_{HRL}, τ_0, and $\Delta\tau$. The physical interpretation, however, becomes much more difficult because now we have to justify both a non-Debye relaxation (finite $\Delta\tau$) of the Li dipoles even in the high-temperature limit and a nonlinear increase of I_{HRL} with x. This requires abandoning the model of almost uncorrelated individual polarization clusters, basic for our attempt to estimate their dipole moment and hyperpolarizability. Thus the very reason for preferring Eqs. (5) and (6) to Eq. (13) is, apart from simplicity, the consistent behavior of the three parameters as functions of x, i.e., $I_{EL}\sim x^2$, $I_{LR}\sim x$, and $\Gamma(x,T)=\Gamma(T)$.

IV. RATIO OF INTEGRATED HYPER-RAYLEIGH AND SOFT-MODE HYPER-RAMAN INTENSITIES

Supposing HRL as well as soft-mode HRM scattering to be described by Eq. (4) with identical coefficients $\partial\chi^{(2)}_{ijk}/\partial P_l^{SM}$, we may complement Eq. (9) by a similar expression for the soft mode, i.e.,

$$S_{SM}(\Omega)\sim[n(\Omega,T)+1]\varepsilon''_{SM}(\Omega), \tag{14}$$

where the factor of proportionality is the same as in Eq. (9) and $\varepsilon''_{SM}(\Omega)$ stands for the imaginary part of the dielectric function of a damped harmonic oscillator. Comparing Eqs. (9) and (14) with Eqs. (5)–(8), we find

$$\frac{I_{LR}}{I_{DHO}}=\frac{k_BT}{\hbar\Omega_0[\tilde{n}(\Omega_0,\gamma,T)+\frac{1}{2}]}\frac{\Delta\varepsilon_D(0)}{\Delta\varepsilon_{SM}(0)}. \tag{15}$$

Here, $\Delta\varepsilon_D(0)=\Delta\varepsilon_D(0,x,T)$ and $\Delta\varepsilon_{SM}(0)=\Delta\varepsilon_{SM}(0,x,T)$ are the contributions of the Debye relaxator and the soft mode to the static dielectric permittivity $\varepsilon(0,x,T)$, respectively. For $\Delta\varepsilon_{SM}(0)$ we may write (cgs units)

$$\Delta\varepsilon_{SM}(0)=4\pi\frac{N}{V}\left(\frac{Z^T_{SM}}{\Omega_0}\right)^2. \tag{16}$$

Following Ref. 27, we have incorporated the square root of the appropriate mass factor into the transverse effective charge Z^T_{SM} of the soft mode. N is the number of unit cells contained in the volume V. Combining Eqs. (15) and (16), we can estimate $\Delta\varepsilon_D(0)$ from the intensity ratio I_{LR}/I_{DHO}. At room temperature, for example, we obtain values ranging from 5 at $x=0.008$ to 47 at $x=0.087$, while $\varepsilon(0,0,T)\approx 240$.[34]

Within the framework of our model, $\Delta\varepsilon_D(0)$ is given by[35]

$$\Delta\varepsilon_D(0)=4\pi\left(\frac{Nx}{V}\right)\frac{(p^*_{PC})^2}{3k_BT} \tag{17}$$

where p^*_{PC} is the external or effective dipole moment of the Li-induced polarization clusters. According to Vugmeister and Glinchuk,[14] p^*_{PC} is defined by the volume integral

$$\vec{p}^*_{PC}=\int\vec{P}_{PC}(\vec{r})d\vec{r}, \tag{18}$$

where $\vec{P}_{PC}(\vec{r})$ is the polarization within the polarization cluster around an individual Li dipole. The intrinsic or true dipole moment p_{PC} differs from p^*_{PC} by a local-field enhancement factor Λ, i.e.,

$$p^*_{PC}=p_{PC}\Lambda. \tag{19}$$

The discussion of Λ will be postponed to Sec. V. As follows from a virial expansion of $\Delta\varepsilon_D(0)$,[36] Eq. (17) is valid as long as $\Delta\varepsilon_D(0)$ remains small compared to $\varepsilon(0,0,T)$. This criterion is satisfied above 230 K.

From Eqs. (15)–(17) we deduce

$$\tilde{I}_{LR}=\frac{I_{LR}}{I_{DHO}}\frac{2\tilde{n}(\Omega_0,\gamma,T)+1}{\Omega_0}=\frac{2}{3\hbar}\left(\frac{p^*_{PC}}{Z^T_{SM}}\right)^2x. \tag{20}$$

In Fig. 8 the quantity $\tilde{I}_{LR}$ is referred to as normalized intensity of the Lorentzian contribution to the HRL line and plotted as a function of x. Values of the effective dipole moment p^*_{PC} obtained by means of Eq. (20) are listed in Table I and will be commented on in the following section.

The local hyperpolarizability β_{ijk} of the Li-induced polarization clusters can be evaluated more directly from the ratio

TABLE I. First-order hyperpolarizability β_{222}, effective dipole moment $p^*_{\rm PC}$, and intrinsic or core dipole moment $p_{\rm PC}$ of Li-induced polarization clusters in $K_{1-x}Li_xTaO_3$ as functions of temperature between 230 and 300 K. The three digits in β_{222} and $p^*_{\rm PC}$ reflect the accuracy of relative values permitting one to detect the temperature dependence of these quantities. Concerning the accuracy of the absolute values see text.

T (K)	β_{222} (10^{-30} g$^{-1/2}$ cm$^{7/2}$ s $\hat{=}4.195\times10^{-40}$ m^4 V^{-1})	p^*_{PC} ($D=10^{-18}$ g$^{1/2}$ cm$^{5/2}$ s^{-1} $\hat{=}(1/3)\times10^{-29}$ C m$=0.208e$ Å)	$p_{\rm PC}$ (D)
229	1.25	23.4	2.3
239	1.21	22.5	2.3
249	1.16	21.7	2.3
259	1.13	21.1	2.3
267	1.10	20.5	2.3
278	1.05	19.6	2.3
300	0.98	18.4	2.3

of HRL and soft-mode HRM intensities. Referring to the scattering geometry $X(YY)Z$, we find

$$\tilde{I}_{\rm LR}=\frac{2}{\hbar}\frac{\langle\tilde{\beta}^2_{222}\rangle\Lambda^2_{\rm opt}}{(\partial\chi^{(2)}_{222}/\partial P^{\rm SM}_2)^2(Z^T_{\rm SM})^2}x, \tag{21}$$

where $\tilde{\beta}_{222}$ is the hyperpolarizability referring to the fixed crystallographic axes and $\Lambda_{\rm opt}$ the *optical* local-field enhancement factor. Whereas Λ in Eq. (19) is difficult to determine because it is large and temperature dependent, its optical counterpart $\Lambda_{\rm opt}$ only represents a correction well approximated by[7]

$$\Lambda_{\rm opt}=\left(\frac{n^2(\omega_L)+2}{3}\right)^2\left(\frac{n^2(2\omega_L)+2}{3}\right). \tag{22}$$

The refractive indices $n(\omega_L)$ and $n(2\omega_L)$ are to be taken at the laser and second-harmonic frequency, respectively. Since the off-center displacements of the Li ions are restricted to the cubic axes, the transformation of the hyperpolarizability from the laboratory to the molecular coordinate system becomes trivial. In the temperature region under study we may assume

$$\langle\tilde{\beta}^2_{222}\rangle=\tfrac{1}{3}\beta^2_{222}, \tag{23}$$

where the tensor element β_{222} refers to a Li ion displaced along the [010] direction. Taking $\partial\chi^{(2)}_{222}/\partial P^{\rm SM}_2$ from Ref. 23, we obtain values of β_{222} also listed in Table I.

V. ABSOLUTE VALUES OF HYPERPOLARIZABILITY AND PERMANENT DIPOLE MOMENT

According to the results of Ref. 29, we expect the high-temperature limit of $\tilde{I}_{\rm LR}$ to follow the proportionality

$$\tilde{I}_{\rm LR}(x,T)\sim x\ \ r^4_c(T). \tag{24}$$

Here, $r_c(T)$ stands for the correlation radius of the soft-mode polarization. With increasing temperature $r_c(T)$ decreases like the inverse soft-mode frequency of the host crystal, so that $\tilde{I}_{\rm LR}$ behaves as $\Omega_0^{-4}(0,T)$. This Ω_0^{-4} law has been predicted and verified for HRL scattering from centrosymmetric perovskites by various authors.[17,37–39] The basic underlying assumption may be summarized in the form

$$\beta\sim\int P_{\rm PC}(\vec{r})d\vec{r}\sim r^2_c, \tag{25}$$

where the volume integral may be replaced by the effective dipole moment of the symmetry-breaking defect according to Eq. (18). Note that in the preceding section we have specified the first proportionality in Eq. (25) by postulating

$$\beta_{222}\Lambda_{\rm opt}=\frac{\partial\chi^{(2)}_{222}}{\partial P^{\rm SM}_2}p^*_{\rm PC} \tag{26}$$

as follows from a comparison of Eqs. (20) and (21). The Ω_0^{-4} law ceases to hold as soon as $2r_c$ approaches the mean distance between neighboring Li ions and neighboring polarization clusters start to touch each other. The ''cluster-coalescence temperature''[29] estimated from this condition is about 150 K at $x=0.043$ and 270 K at $x=0.087$. Experimentally, however, Eq. (24) is confirmed down to below 230 K for all six samples under study. In Table I the temperatures are restricted to a range where the Lorentzian contribution to the HRL line can clearly be separated from the unresolved elastic one and $\tilde{I}_{\rm LR}$ satisfies Eq. (24).

The absolute value of β_{222} reaches the order of magnitude of the first-order hyperpolarizability of medium-sized organic molecules like aniline or nitrobenzene, i.e., 10^{-30} g$^{-1/2}$cm$^{7/2}$s corresponding to 3.7×10^{-51} C V^{-2} m^3 in SI units or to 4.2×10^{-40} m^4 V^{-1} if the permittivity of free space is included in the right-hand side of Eq. (1).[1–6] The uncertainty of the *absolute* values of β_{222} is mainly determined by that of the EFISHG coefficient used for calibration according to Eq. (21) and hence becomes as large as $\pm30\%$.[21] This inaccuracy, however, does not obscure the temperature dependence of β_{222} clearly revealed in Table I because the *relative* values of β_{222} only require the knowledge of the intensity ratio $\tilde{I}_{\rm LR}$ as a function of x and have experimental errors of less than $\pm10\%$. Similar remarks apply to the effective dipole moment $p^*_{\rm PC}$. Again, the variation with temperature shown in Table I does not become obsolete due to the uncertainty of the *absolute* values of $p^*_{\rm PC}$ which,

however, is considerably smaller than that of the absolute values of β_{222} since the transverse effective charge used for calibration according to Eq. (20) is known within experimental errors of about $\pm 5\%$.[27,34]

Table I confirms the proportionalities

$$\beta_{222}(T) \sim p^*_{\mathrm{PC}}(T) \sim \Omega_0^{-2}(0,T) \sim \varepsilon(0,0,T) \tag{27}$$

expected from Eqs. (25) and (26). This result suggests to use the expression

$$\Lambda = \frac{\eta}{3}\left[\varepsilon(0,0,T) + \frac{3}{\eta} - 1\right] \approx \frac{\eta}{3}\varepsilon(0,0,T) \tag{28}$$

for the local-field enhancement factor in Eq. (19) as has been done by Vugmeister *et al.*[14,40] Here, η indicates the reduced coupling between the Li dipole and the soft-mode polarization as evidenced by the well-known fact that the K sublattice does not participate appreciably in the soft-mode vibration. Some information about η can be gained by calculating the prefactor in the Lorentz field at the K site in pure $KTaO_3$ and writing it in the form $(4\pi/3)\eta$. Various estimates have yielded $\eta < 0$ and $|\eta| \approx 0.1$.[14] Inserting Eq. (28) in Eq. (19), we obtain the temperature-independent values $|\eta| p_{\mathrm{PC}} = 0.23$ D or $p_{\mathrm{PC}} \approx 2.3$ D. Our estimates are smaller by a factor of 1.7 than those derived from the x dependence of the phase transition temperature below 100 K predicted by the model of soft-mode mediated dipole-dipole interaction.[14,40] However, in view of the various assumptions necessary to arrive at absolute values of $|\eta| p_{\mathrm{PC}}$ or p_{PC} both by HRM spectroscopy and by model calculation, we cannot expect more than an order of magnitude agreement. We also refrain from arguing that our value of p_{PC} supports recent computer simulations[22,41] yielding a Li off-center displacement $\delta_{\mathrm{Li}} \approx 0.6$ Å that is much smaller than the values $\delta_{\mathrm{Li}} = 1.26$ Å or even $\delta_{\mathrm{Li}} = 1.45$ Å deduced from NMR and x-ray data, respectively.[42,43] In using Eq. (28) we obtain the certainly correct result that the dipole moment p_{PC} at the core of the polarization cluster is independent of temperature. However, no information is gained about the size of the core, so that it is not well justified to identify p_{PC} with the dipole moment of the bare off-center Li ion. In order to calculate δ_{Li} from the effective dipole moment p^*_{PC} accessible to HRM spectroscopy, we need a more detailed analysis of the polarization cluster combining an atomistic treatment of the core with refined descriptions of the polarization $\vec{P}_{\mathrm{PC}}(\vec{r})$ in the outer region.

VI. SUMMARY

In the temperature interval between 200 and 300 K the thermally activated hopping motions of the Li ions in $K_{1-x}Li_xTaO_3$ lead to a spectral broadening of the HRL line resolvable even with a spectral slit width of 2.7 cm^{-1}. Thus the relaxation frequencies of the Li subsystem have now been shown to sweep through the whole range between 10^{-3} and 10^{11} Hz on heating from the glass or ferroelectric-type phase transition point to room temperature. Attention is focused on the Lorentzian component of the HRL line characterized by a linewidth Γ independent of x and an intensity I_{LR} proportional to x. The behavior of Γ and I_{LR} is interpreted as evidence that the high-temperature limit has been reached where the orientational correlations between the Li dipoles may be ignored. In modifying the internal reference method for determining first-order hyperpolarizabilities of molecules in solution, we use the soft-mode HRM line as an intensity standard for calibrating I_{LR}. Absolute values of the local hyperpolarizability β and the effective dipole moment p^*_{PC} of the Li ions including their surrounding polarization clusters are estimated from ratios of HRL and HRM intensities. The temperature dependence of both quantities is shown to indicate the growth of the polarization clusters with decreasing temperature. The problem remains to relate the effective dipole moment p^*_{PC} to the intrinsic one p_{PC}, which has to be attributed to the core of the polarization cluster. Taking the common local-field enhancement factor modified by Vugmeister *et al.*,[14] we obtain the temperature-independent value $p_{\mathrm{PC}} = 2.3$ D.

There are several directions in which the present work has to be continued:

(a) An improved spectral resolution should permit one to study the HRL broadening down to temperatures where the linewidth Γ starts to vary with x, indicating the onset of cooperative behavior.

(b) The hypothesis that the soft-mode HRM tensor also controls HRL scattering can be tested by comparing the values of $\Delta\varepsilon_D(0)$ determined by means of Eq. (15) with those supplied by direct dielectric measurements at high temperatures.

(c) The yet unresolved component of the HRL line deserves further investigation in order to confirm that it arises from closely spaced Li pairs and correlates with the second, higher-barrier relaxation process.

Attempts in these directions are in progress.

ACKNOWLEDGMENTS

The author is much indebted to S. Kapphan for providing the samples of KLT. He also thanks W. Kress for a critical reading of the manuscript.

[1] K. Clays, A. Persoons, and L. DeMaeyer in *Modern Nonlinear Optics*, Part 3, edited by M. Evans and S. Kielich, Advances in Chemical Physics, Vol. 85 (John Wiley & Sons, New York, 1994), p. 455.

[2] S. Stadler, G. Bourhil, and C. Bräuchle, J. Phys. Chem. **100**, 6927 (1996).

[3] P. Kaatz and D.P. Shelton, Rev. Sci. Instrum. **67**, 1438 (1996).

[4] K. Clays and A. Persoons, Phys. Rev. Lett. **66**, 2980 (1991).

[5] M. Kauranen and A. Persoons, J. Chem. Phys. **104**, 3445 (1996).

[6] D. Pugh and J.O. Morley, in *Nonlinear Optical Properties of Organic Molecules and Crystals*, Vol. 1, edited by D.S. Chemla and J. Zyss (Academic Press, Orlando, 1987), p. 193.

[7] J.L. Oudar and H. Le Person, Opt. Commun. **15**, 258 (1975).
[8] J.J. van der Klink, D. Rytz, F. Borsa, and U.T. Höchli, Phys. Rev. B **27**, 89 (1983).
[9] U.T. Höchli, Phys. Rev. Lett. **48**, 1494 (1982).
[10] U.T. Höchli and M. Maglione, J. Phys.: Condens. Matter **1**, 2241 (1989).
[11] H.M. Christen, U.T. Höchli, A. Châtelain, and S. Ziolkiewicz, J. Phys.: Condens. Matter **3**, 8387 (1991).
[12] F. Wickenhöfer, W. Kleemann, and D. Rytz, Ferroelectrics **135**, 333 (1992).
[13] P. Doussineau, Y. Farssi, C. Frénois, A. Levelut, K. McEnaney, J. Toulouse, and S. Ziolkiewicz, Phys. Rev. Lett. **70**, 96 (1993); Europhys. Lett. **24**, 415 (1993).
[14] B.E. Vugmeister and N.D. Glinchuk, Rev. Mod. Phys. **62**, 993 (1990).
[15] U.T. Höchli, K. Knorr, and A. Loidl, Adv. Phys. **39**, 405 (1990).
[16] W. Kleemann, Int. J. Mod. Phys. B **7**, 2469 (1993).
[17] H. Vogt, Phys. Rev. B **41**, 1184 (1990).
[18] H. Vogt, J. Phys.: Condens. Matter **3**, 3697 (1991).
[19] B. Salce, J.L. Gravil, and L.A. Boatner, J. Phys.: Condens. Matter **6**, 4077 (1994).
[20] I.P. Bykov, M.D. Glinchuk, V.V. Laguta, J. Rosa, and L. Jastrabik, Ferroelectrics **184**, 285 (1996).
[21] Y. Fujii and T. Sakudo, Phys. Rev. B **13**, 1161 (1976).
[22] R.I. Eglitis, A.V. Postnikov, and G. Borstel, Phys. Rev. B **55**, 12 976 (1997).
[23] H. Vogt, Phys. Rev. B **36**, 5001 (1987).
[24] G.A. Azzini, G.P. Banfi, E. Giulotto, and U.T. Höchli, Phys. Rev. B **43**, 7473 (1991).
[25] P. Voigt and S. Kapphan, J. Phys. Chem. Solids **55**, 853 (1994).
[26] A.D. Bruce and R.A. Cowley, Adv. Phys. **29**, 219 (1980), especially Sec. III.5.2.1.
[27] H. Vogt, Phys. Rev. B **38**, 5699 (1988).
[28] H. Vogt, Phys. Rev. B **51**, 8046 (1995).
[29] H. Vogt, J. Phys.: Condens. Matter **7**, 5913 (1995).
[30] H. Vogt, Ferroelectrics **184**, 31 (1996); **202**, 157 (1997).
[31] A.O. Caldeira and A.J. Leggett, Ann. Phys. (N.Y.) **149**, 374 (1983), Appendix B.
[32] H. Vogt and G. Rossbroich, Phys. Rev. B **24**, 3086 (1981).
[33] V. Trepakov, F. Smutný, V. Vikhnin, V. Bursian, L. Sochava, L. Jastrabik, and P. Syrnikov, J. Phys.: Condens. Matter **7**, 3765 (1995).
[34] H. Vogt and H. Uwe, Phys. Rev. B **29**, 1030 (1984).
[35] H. Fröhlich, *Theory of Dielectrics* (Clarendon Press, Oxford, 1968), Chap. II.
[36] B.E. Vugmeister and V.A. Stefanovich, Fiz. Tverd. Tela **27**, 2034 (1985) [Sov. Phys. Solid State **27**, 1220 (1985)].
[37] A.P. Levanyuk, A.I. Morozov, and A.S. Sigov, Fiz. Tverd. Tela **28**, 436 (1986) [Sov. Phys. Solid State **28**, 242 (1986)].
[38] W. Prusseit-Elffroth and F. Schwabl, Appl. Phys. A: Solids Surf. **51**, 361 (1990).
[39] K. Inoue, A. Yamanaka, A. Hasegawa, and H. Yamaguchi, Ferroelectrics **156**, 297 (1994).
[40] B.E. Vugmeister and V.A. Stephanovitch, Solid State Commun. **63**, 323 (1987); Zh. Éksp. Teor. Fiz. **97**, 1867 (1990) [Sov. Phys. JETP **70**, 1053 (1990)].
[41] M. Exner, C.R.A. Catlow, H. Donnerberg, and O.F. Schirmer, J. Phys.: Condens. Matter **6**, 3379 (1994).
[42] J.J. van der Klink and F. Borsa, Phys. Rev. B **30**, 52 (1984).
[43] E.A. Zhurova, V.E. Zavodnik, and V.G. Tsirelson, Kristallografiya **40**, 816 (1995) [Crystallogr. Rep. **40**, 753 (1995)].